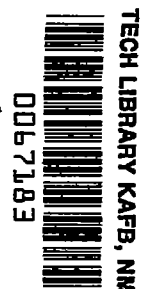


10753  
NACA TN 4409



# NATIONAL ADVISORY COMMITTEE FOR AERONAUTICS

TECHNICAL NOTE 4409

FLIGHT MEASUREMENTS OF THE VIBRATION EXPERIENCED BY A  
TANDEM HELICOPTER IN TRANSITION, VORTEX-RING STATE,  
LANDING APPROACH, AND YAWED FLIGHT

By John E. Yeates

Langley Aeronautical Laboratory  
Langley Field, Va.



Washington  
September 1958

TECHNICAL NOTE 4409



## TECHNICAL NOTE 4409

FLIGHT MEASUREMENTS OF THE VIBRATION EXPERIENCED BY A  
TANDEM HELICOPTER IN TRANSITION, VORTEX-RING STATE,  
LANDING APPROACH, AND YAWED FLIGHT

By John E. Yeates

## SUMMARY

As part of a general program of helicopter vibration research, a flight investigation involving several flight maneuvers that are critical with respect to vibration has been conducted. The maneuvers include transition near the ground, landing approaches, vortex-ring state, and yawed forward flight.

For the transition region the peak vibration occurs in the forward-speed range where the interference induced flow is expected to be rapidly changing and might be expected to influence vibration. The vibration measured in the vortex-ring state is characterized by a large irregular pulsing of the vibration envelope at a random frequency, which probably indicates shedding of the vortices. The vibration experienced during a landing approach can be markedly reduced by choosing a rotor speed which minimizes the coupling of the structural components. In forward flight at 40 knots the vibration is reduced by a factor of about 3 at the rear rotor and is only slightly reduced at the front rotor when the helicopter is yawed to an angle of about  $23^{\circ}$ .

## INTRODUCTION

The magnitude of the vibrations in some of the larger helicopters has made these machines unacceptable for commercial or military operations. With some of the helicopters in current use, the vibrations are tolerated but are very objectionable to the pilot and passengers. These vibrations also affect flight safety, particularly from a structural fatigue standpoint, as well as inducing pilot and passenger fatigue and discomfort.

During the flight program of reference 1, large-magnitude vibrations were noted in flight conditions involving transition, vortex-ring state, and landing approaches. The nearness of the rotor rotational

frequency to the uncoupled fuselage resonant frequency results in the large amount of 3-per-revolution vibration (designated herein as 3-P) present in flight. Because these vibrations are of considerable importance from a structural and pilot fatigue standpoint, they were the subject of further study, the results of which are reported herein.

It has been known for some time that for carrier guard duty, helicopter pilots fly their machines at some yaw angle to lessen the effects of vibration. The variation of vibration with yaw angle in forward flight was thought to be of interest in that, at some yaw angle, vibration due to interference between rotors appears to be minimized. The results of this investigation are discussed herein.

#### SYMBOLS

$x$	vibratory amplitude, in.
$\dot{x}$	vibratory velocity, in./sec
$\omega$	frequency, radians/sec
3-P	3-per-revolution frequency, cps
$v$	average induced velocity in hovering, ft/sec
$V_v$	rate of descent, ft/min
$\overline{V_v}$	nondimensional rate of descent, $V_v/v$
$q$	pitching velocity (positive nose up), radians/sec

#### EQUIPMENT AND INSTRUMENTATION

##### Helicopter

A tandem helicopter with three-blade rotors was used for the investigation. (See fig. 1.) The helicopter was equipped with production metal blades for the tests. The mass and stiffness distributions of the blades are shown in figure 2.

## Instrumentation

The test helicopter was instrumented for a general helicopter vibration study. (See ref. 1 for details.) Motions of the structure were measured by means of velocity-type vibration pickups. In this paper, only measurements at the front and rear rotors in a vertical direction are reported. Time histories of the output of the velocity pickups were recorded by an oscillograph. The velocity-pickup—oscillograph combinations have response curves which are similar to that of figure 3. Since the curves show about 95 percent response at the 3-P frequency, no response corrections have been applied to the data. The flight conditions (airspeed, altitude, angle of yaw, etc.) were obtained through use of standard NACA recording instruments synchronized with the oscillograph through a common timing circuit.

## Analysis Equipment

The frequency-analysis equipment consisted of a two-channel variable-filter-width heterodyne harmonic analyzer and associated playback and recording equipment. The analyzer provides a reading of the mean square of the signal passed by a tunable filter with an accuracy of  $\pm \frac{1}{2}$  decibel.

For the analysis it was necessary to transcribe the oscillograph records onto magnetic tape. In order to obtain a time history of the frequency component of interest, namely the 3-P component at 13.5 cps, the filter was set at this frequency and the tape record was run through the analyzer. The component time history was recorded on an oscillograph.

The absolute accuracy with which the center frequency of the filter is known is estimated to be within 2 cps. For the present investigation, the data were analyzed at 10 times normal tape speed and therefore the center frequency is known to within 0.20 cps. The band width of the filter used for the data analysis was about 1 cps in true time.

## TESTS AND ANALYSIS

### Tests

Transition.— Transition is a term generally used to refer to a flight condition intermediate between hovering and the speed for minimum power, and is defined in this report as the speed region from 10 to 30 knots. It is well known that for most helicopters the vibration

spectrum over the speed range has two regions of large-magnitude vibration - one in the transition region and the other in the region of blade stall. Transition is loosely used herein to refer to the speed range where vibration first reaches a maximum.

The flight plan for this portion of the tests consisted of climbing or descending at about 150 ft/min while traversing the transition region. The peak level of vibration encountered in this region depends upon the rate of traverse of the range from 10 to 30 knots. For the data presented, the rate of traverse of this speed range was slow enough to allow the vibration to build up to a maximum. For the descent condition, the pilot executed a gradual flare at about the same time that the helicopter was passing through the transition region.

Landing approaches.- For all the landing approaches, the rotor speed was set at a predetermined value and a straight-in airplane type of approach, at a rate of descent of about 150 ft/min, was established. When within a rotor diameter of the ground, the pilot executed a flare to hover.

Vortex-ring state.- As soon as a rotor starts to descend from hovering, a definite slipstream - extending from far above to far below the rotor - ceases to exist. At low rates of descent the resultant flow through the disk is still downward because of the large induced velocity, but the flow far above the rotor is upward. The defined limits of the vortex-ring state are hovering and the condition where the rate of descent is equal to twice the average induced velocity. The vortex-ring state is characterized by large recirculating flows and the absence of a definite slipstream. (See ref. 2.)

The flight plan for this maneuver consisted of maintaining a constant rotor speed while hovering or at a forward speed of 10 knots and then reducing power until the helicopter started to descend. In this flight condition the helicopter appeared to "wallow" around while the rate of descent steadily increased. The pilot recovered from the maneuver by pushing the nose down and increasing forward speed.

Yawed flight.- The flight plan for yawed flight consisted of maintaining altitude, constant power and rotor speed, and approximately constant forward speed (40 knots), and then yawing the helicopter to the right and left at about 150 deg/min up to an angle of yaw of about 23°.

### Analysis

In the analysis the vibration data were handled in two ways. For the first method, the vibration records containing all frequency components were read in terms of vibratory velocity by applying the normal

instrument calibration factor. For the second method, the oscillograph records were transcribed onto magnetic tape and the data were analyzed by analog frequency-analysis methods. Time histories of the vibration component of interest (3-P) were recorded on an oscillograph. These time-history records were read at discrete points, and by means of a suitable calibration the data were tabulated in terms of velocity vector. These data were then converted to displacement by the relation  $x = \dot{x}/\omega$ .

## RESULTS AND DISCUSSION

### Transition Near the Ground

Climb.- In figure 4 are shown time histories of the vertical vibration (containing all frequency components) measured at the front and rear rotors along with some of the flight conditions which are indicative of the dynamics of a shallow-climb maneuver. It can be seen from the figure that the envelope of vibration reaches a maximum near a forward speed of 20 ft/sec for both rotors. This peaking of the vibration occurs in a forward-speed region where the interference induced flow is expected to be rapidly changing and might be expected to influence vibration. The theory of references 3 and 4 was used in an attempt to correlate the change in the asymmetry of the interference-induced-flow distributions with vibration. However, there did not appear to be any detailed correlation.

Descent.- In figure 5 are shown time histories of the vertical vibration (containing all frequency components) measured at the front and rear rotors along with some of the flight conditions which are indicative of a dynamic maneuver. The figure shows that the vibration reaches a maximum near a forward speed of 17 ft/sec for both rotors. The vibration again peaks in the forward-speed region where the interference induced flow is expected to be rapidly changing and might be expected to influence vibration. An attempt was again made to obtain a detailed correlation of the change in the asymmetry of the interference-induced-flow distributions with vibration, but was unsuccessful. The descent is complicated by the fact that the flare is accomplished at approximately the same time that the maximum vibration occurs. It can be seen by comparing figures 4 and 5 that the peak levels of the vibration envelopes in figure 5 are higher than the peak levels in figure 4. It is believed that the difference in the peak levels of vibration in figures 4 and 5 is primarily the result of the flare.

The vibration encountered in the transition region is considered to be the most critical for this helicopter. In order to compare the relative magnitudes of the aerodynamic forcing for the transition region and for a low-vibration condition (level flight at 55 knots), figures 5 and 6

are presented. It can be seen in the figures that the peak level of vibration at the rear rotor is nearly four times as large in transition as in level flight. A similar result was noted for the front rotor.

### Effect on Vibration of Nearness of Rotor Speed to Fuselage Resonance During Landing

#### Approach Maneuvers

Landing approach maneuvers were executed to determine whether the same trend in vibration coupling with rotor speed exists during a high-level vibration maneuver as was noted in reference 1 during cruise flight at minimum vibration.

Comparisons of the 3-P component of vertical vibration measured at the front and rear rotors for rotor speeds of 290, 273, and 250 rpm during landing approach maneuvers are shown in figure 7. For a rotor speed of 290 rpm, it can be seen that the 3-P component of vibration reaches a peak of about 0.06 inch at the rear rotor and 0.045 inch at the front rotor near a forward speed of 27 ft/sec. For a rotor speed of 273 rpm, the 3-P vibration reaches a peak of about 0.11 inch at the rear rotor and 0.09 inch at the front rotor near a forward speed of 25 ft/sec. For a rotor speed of 250 rpm, the 3-P vibration reaches a peak of about 0.175 inch at the rear rotor and 0.095 inch at the front rotor at a forward speed near 20 ft/sec. Thus, in figure 7, a general trend is noted; as rotor speed is decreased from 290 to 250 rpm and brought nearer to fuselage resonance, the peak vibration increases by a factor of 2 or more. This change in vibration level due to change in rotor speed is primarily a result of resonance amplification, as is pointed out in reference 1. The same type of vibration coupling is apparently present during high-level-vibration landing approaches as was present in cruise flight near minimum vibration conditions. Thus, the importance of avoiding coupled-frequency resonance conditions by a combination of design and operational practices is again illustrated.

#### Vortex-Ring State

As was previously mentioned, the vortex-ring state is characterized by large recirculating flows and the absence of a definite slipstream. The defined limits of the vortex-ring state are hovering and the condition where the rate of descent is equal to twice the average induced velocity in hovering ( $2v$ ). In order to illustrate the character of the vibration near a value of  $\overline{V_v}$  of zero, figure 8 is presented. The regular nature of the vibration envelope can be observed. From oscillograph records, the observable occurrence of the vortex-ring state

(pulsative character of the vibration envelope) appears to extend between values of  $\bar{V}_V$  of about -0.23 and -1.25 near zero forward speed. When  $\bar{V}_V$  increases to more than -1.25, the vibration envelope again becomes regular (pilots' opinion).

Descent with forward speed near zero.- In figure 9 are shown time histories of the vibration envelopes (containing all frequency components of vibration) measured at the front and rear rotors for a rate of descent which varies from 360 ft/min ( $\bar{V}_V = -0.23$ ) to 1,940 ft/min ( $\bar{V}_V = -1.25$ ) during the record. The vibration envelopes at the front and rear rotors are characterized by large irregular peaks, especially near a rate of descent of 1,600 ft/min ( $\bar{V}_V = -1.03$ ). The vibration envelopes seem to pulse at a random frequency that appears to vary in response to the irregular shedding of vortices, which is discussed in reference 5. This pulsating of the vibration envelope is not a result of pilot-induced control motions nor is it associated with rotor frequency. As the rate of descent starts to increase from 360 ft/min ( $\bar{V}_V = -0.23$ ), the vibration increases and reaches a peak near 1,600 ft/min ( $\bar{V}_V = -1.03$ ). When the rate of descent further increases to about 1,950 ft/min ( $\bar{V}_V = -1.25$ ), the helicopter appears to have reached the end of the observable effects of the vortex-ring state (pilots' opinion).

Descent with forward speed near 10 knots.- Figure 10 presents time histories of the vibration envelopes (containing all frequency components) measured at the front and rear rotors for a rate of descent which ranged from 500 ft/min ( $\bar{V}_V = -0.32$ ) to 1,150 ft/min ( $\bar{V}_V = -0.74$ ) near 10 knots. A forward speed of 10 knots appears to be near the limiting speed for the observable effect of the vortex-ring state. The pulses in the vibration envelopes of figure 10 have a more regular occurrence with forward speed than those of figure 9, possibly indicating a more regular shedding of vortices. It can also be noted in figure 10 that the mean level of vibration is changed as forward speed is increased. A comparison of figures 9 and 10 shows that when forward speed is increased to 10 knots while the helicopter is in the vortex-ring state, the mean level of vibration is increased for the rear rotor and is decreased for the front rotor. The pilot noted that control was much easier with forward speed.

#### Yawed Flight

In figure 11 are shown plots of vertical vibration (containing all frequency components) at the front and rear rotors for a range of yaw angles as the helicopter is yawed to the left in forward flight at 40 knots. The vibration at the front rotors appears to be reduced only slightly as the yaw angle is increased to a maximum of approximately  $23^\circ$ . The vibration at the rear rotor, however, is reduced to about one-third



of what it was at the beginning of the maneuver. When yaw angle was further increased, the vibration was observed to increase (pilots' opinion) from its low level at  $23^{\circ}$ . Similar records showed that when the helicopter was yawed to the right, a similar decrease in vibration occurred at the rear rotor, but again the vibration at the front rotor was only slightly decreased. It thus appears that when the helicopter is yawed to the left or right near a forward speed of 40 knots, a reduction occurs in the interference effect between the front and rear rotors. Thus the vibration at the rear rotor is greatly decreased.

The maneuver just described has been practiced by helicopters on carrier guard duty for some time. It appears to be effective for this rotor arrangement and might be expected to be effective for most tandem helicopters.

#### CONCLUDING REMARKS

Several types of flight maneuvers that are critical with respect to vibration have been made in a tandem helicopter. The maneuvers include transition near the ground, landing approaches, vortex-ring state, and yawed forward flight.

In the transition region, the peak vibration occurs in the forward-speed range where the interference induced flow is expected to be rapidly changing and might be expected to influence vibration.

In the vortex-ring state the vibration is characterized by a large irregular pulsating of the vibration envelope at a random frequency, which is probably the result of shedding of vortices. The vibration reaches a maximum for zero forward speed near a rate of descent of 1,600 ft/min, and for a forward speed of 10 knots reaches a maximum near a rate of descent of 1,150 ft/min.

The overall vibration can be appreciably reduced by flying the helicopter in yawed forward flight. The vibration at the rear rotor was reduced by a factor of about 3 while that at the front rotor was only slightly reduced at a yaw angle of  $23^{\circ}$  and a forward speed of 40 knots. The mechanism which causes a reduction in vibration with yaw angle is believed to be interference flow.

Langley Aeronautical Laboratory,  
National Advisory Committee for Aeronautics,  
Langley Field, Va., August 26, 1958.

## REFERENCES

1. Yeates, John E., Jr., Brooks, George W., and Houbolt, John C.: Flight and Analytical Methods for Determining the Coupled Vibration Response of Tandem Helicopters. NACA Rep. 1326, 1957. (Supersedes NACA TN 3852 by Yeates and TN 3849 by Brooks and Houbolt.)
2. Gessow, Alfred, and Myers, Garry C., Jr.: Aerodynamics of the Helicopter. The Macmillan Co., c.1952.
3. Heyson, Harry H., and Katzoff, S.: Induced Velocities Near a Lifting Rotor With Nonuniform Disk Loading. NACA Rep. 1319, 1957. (Supersedes NACA TN 3690 and TN 3691.)
4. Castles, Walter, Jr., and DeLeeuw, Jacob Henri: The Normal Component of the Induced Velocity in the Vicinity of a Lifting Rotor and Some Examples of Its Application. NACA Rep. 1184, 1954. (Supersedes NACA TN 2912.)
5. Drees, J. Meijer, and Hendal, W. P.: The Field of Flow Through a Helicopter Rotor Obtained From Wind Tunnel Smoke Tests. Rep. A. 1205, Nationaal Luchtvaartlaboratorium (Amsterdam), Feb. 1950.

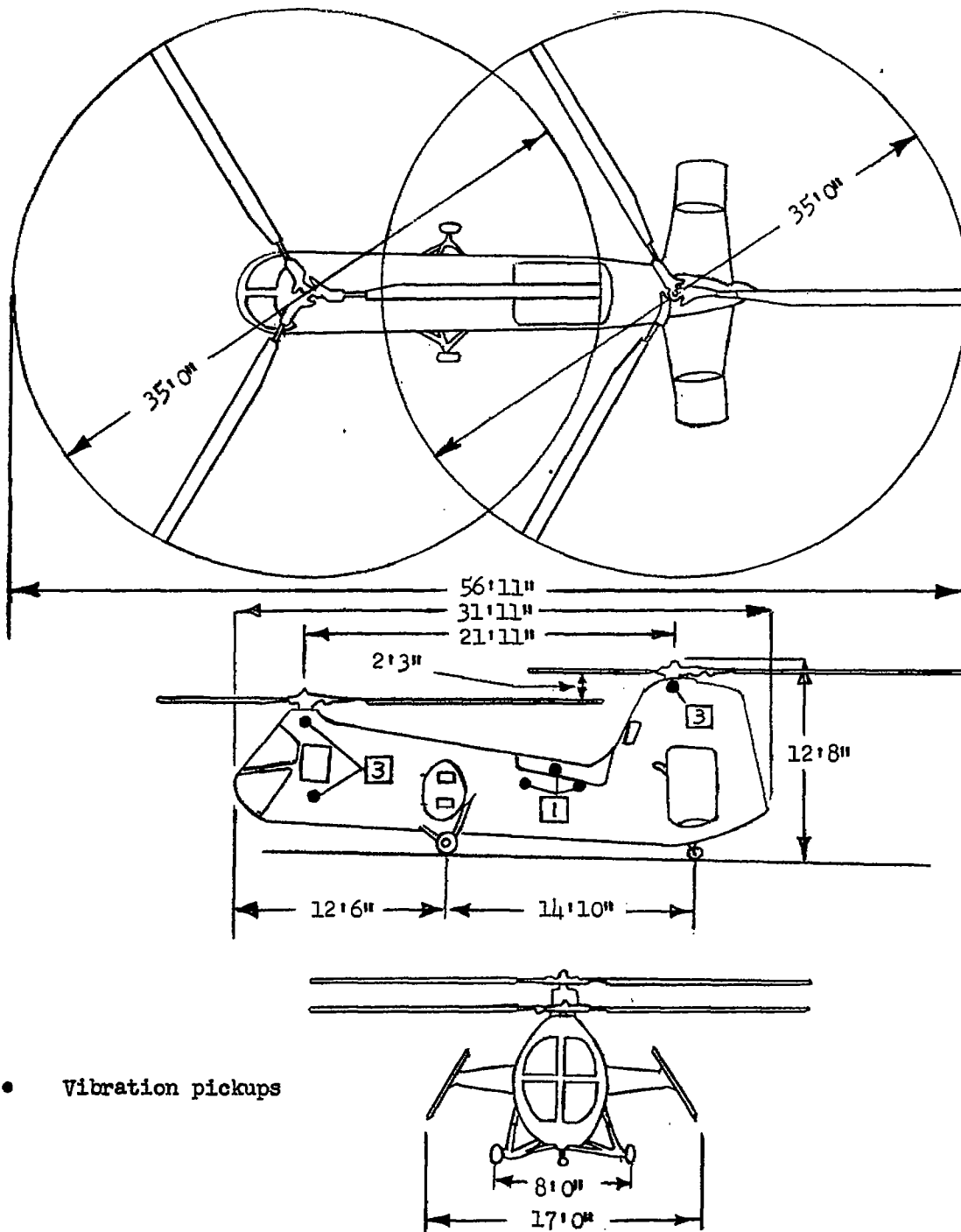


Figure 1.- Test helicopter showing location of vibration pickups and number of components measured.

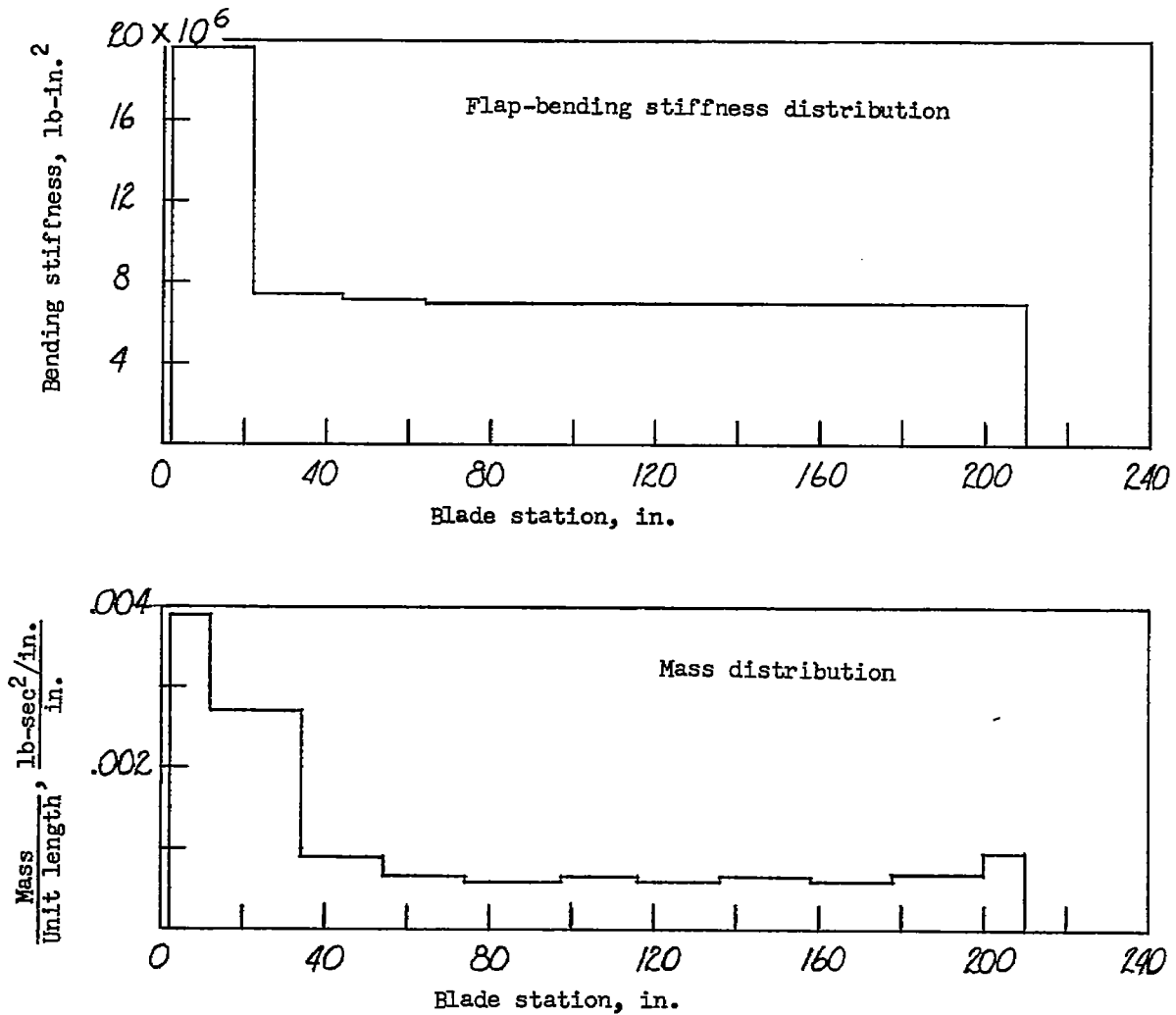


Figure 2.- Mass and stiffness characteristics of the blades used for the tests (natural frequency of nonrotating blades, 5.5 cps).

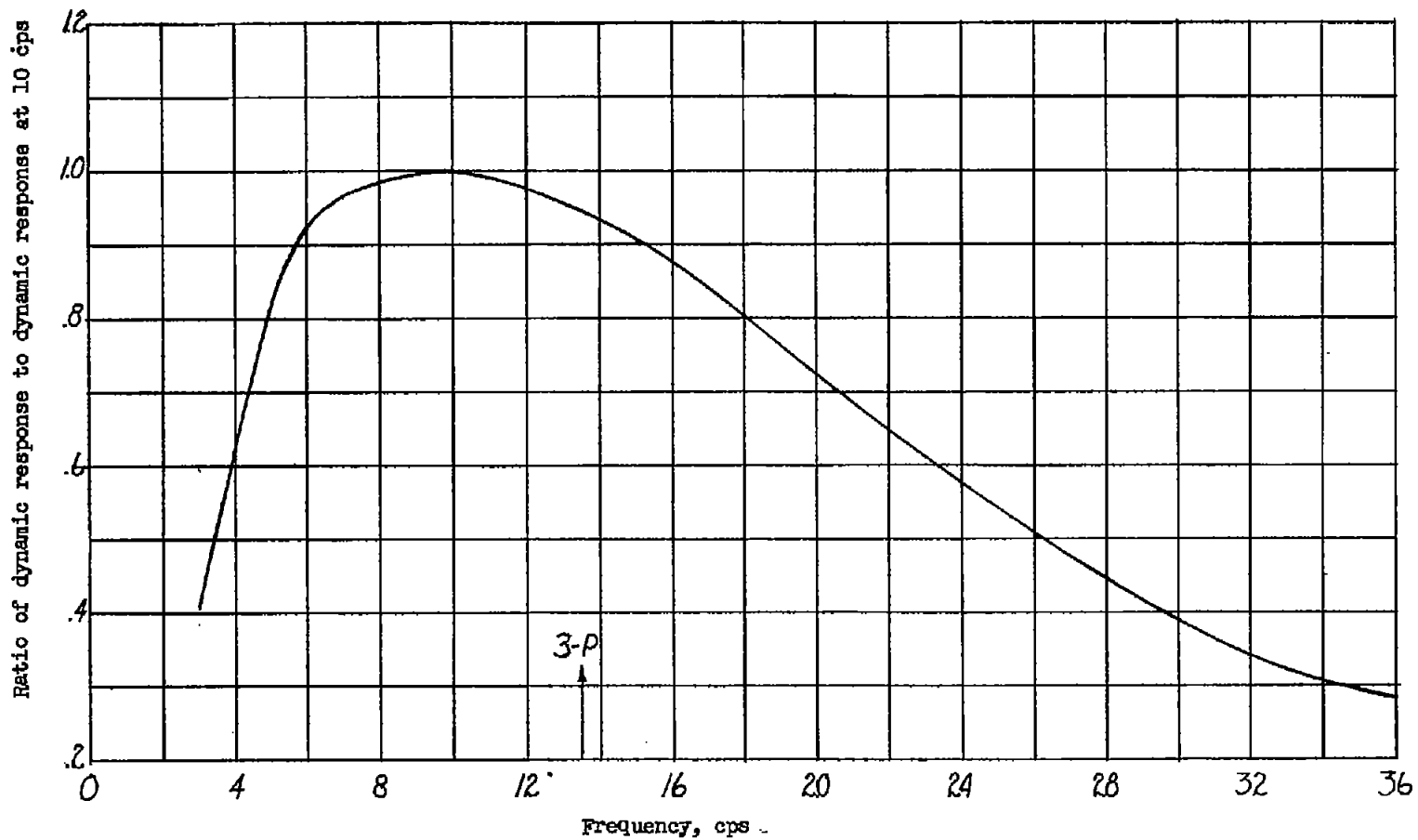


Figure 3.- Typical response curve for vibration-pickup—oscillograph combination used.

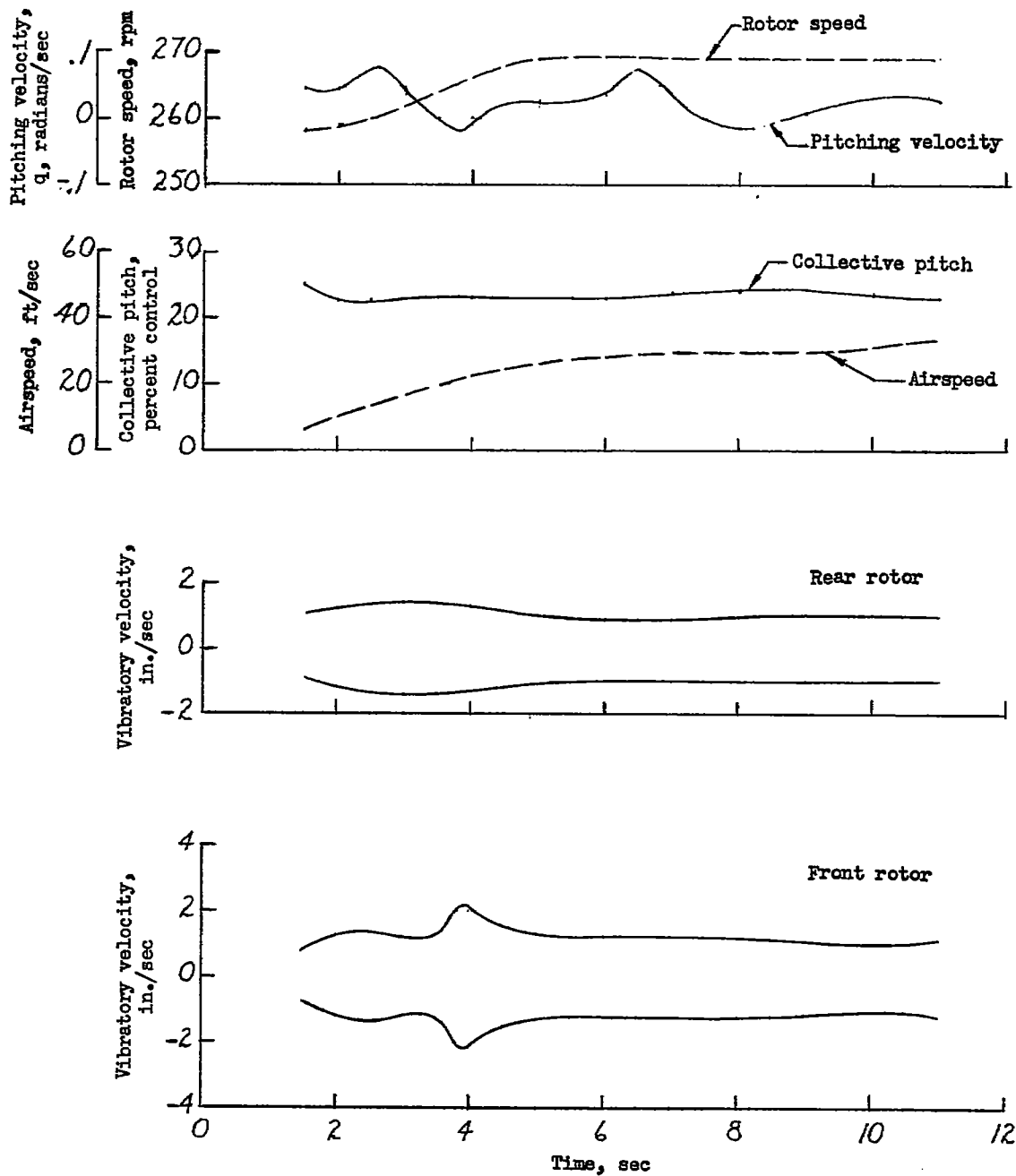


Figure 4.- Time history of the envelopes of vertical vibration (containing all frequency components) measured at the front and rear rotors and flight conditions during a shallow climb through transition.

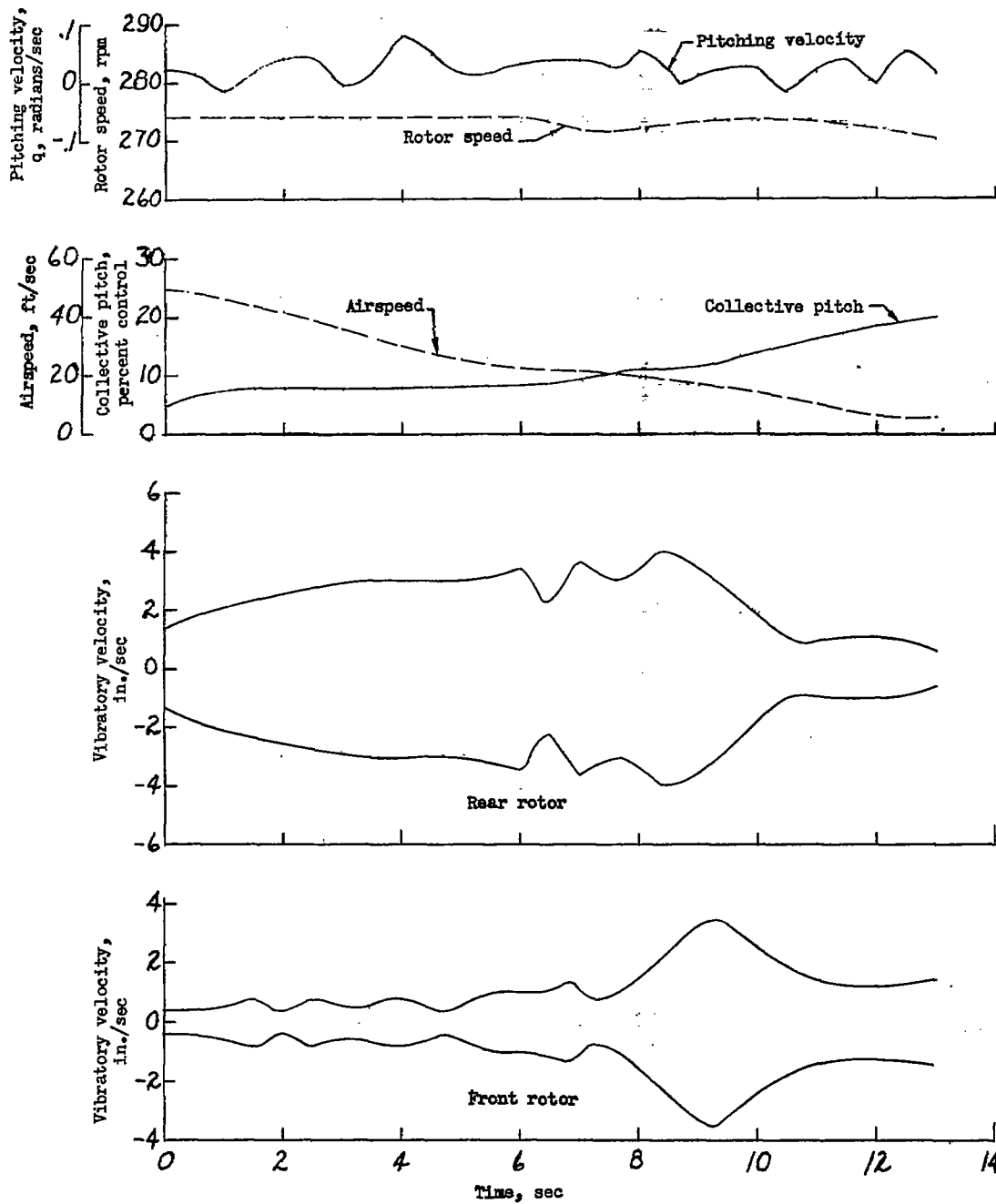


Figure 5.- Time history of the envelopes of vertical vibration (containing all frequency components) measured at the front and rear rotors and flight conditions during gradual descent through transition.

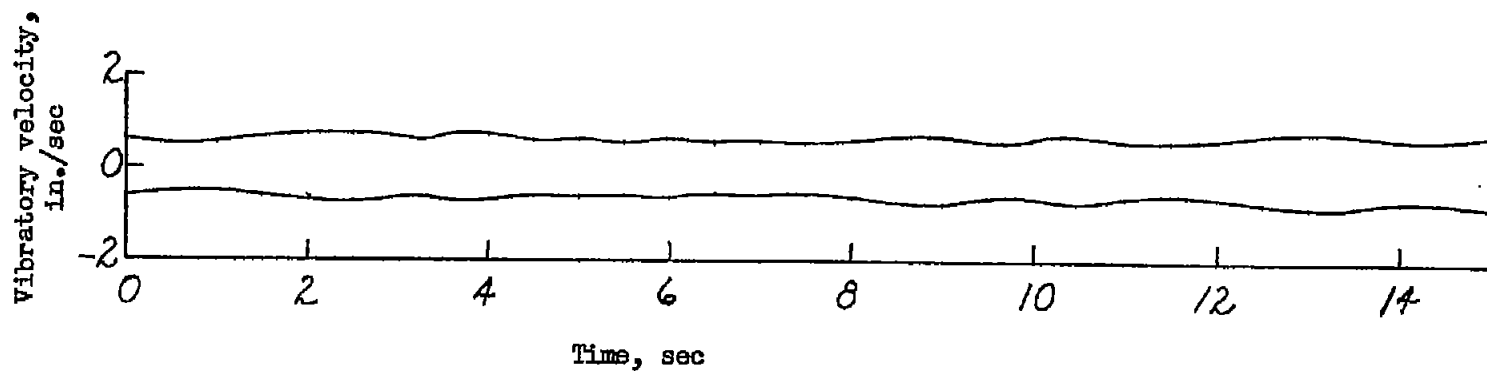


Figure 6.- Time history of the envelope of vertical vibration (containing all frequency components) at the rear rotor during level flight at a forward speed of 55 knots.



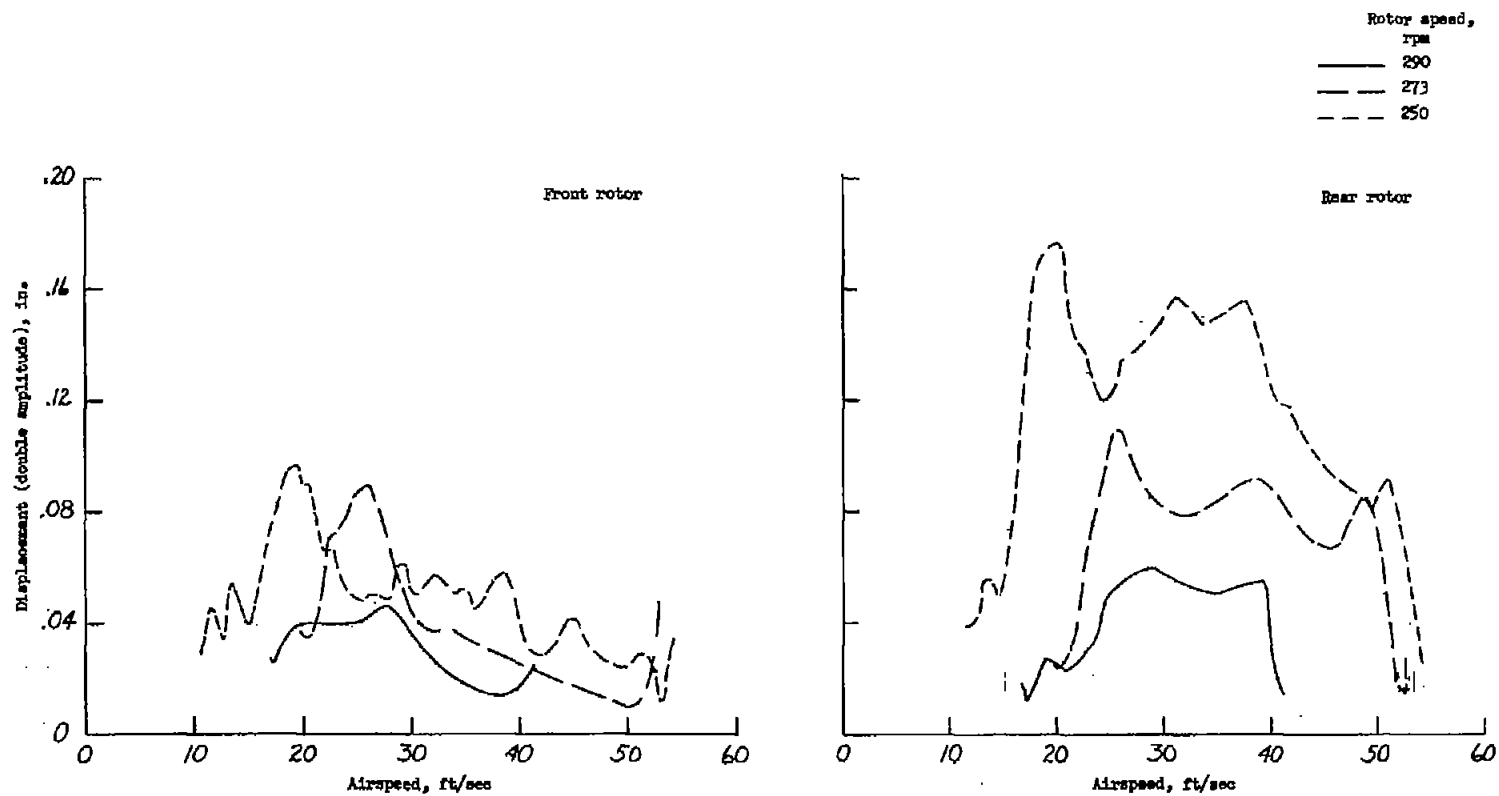


Figure 7.- Variation of the 3-P component of vertical vibration with airspeed during landing approach maneuvers for several rotor speeds.

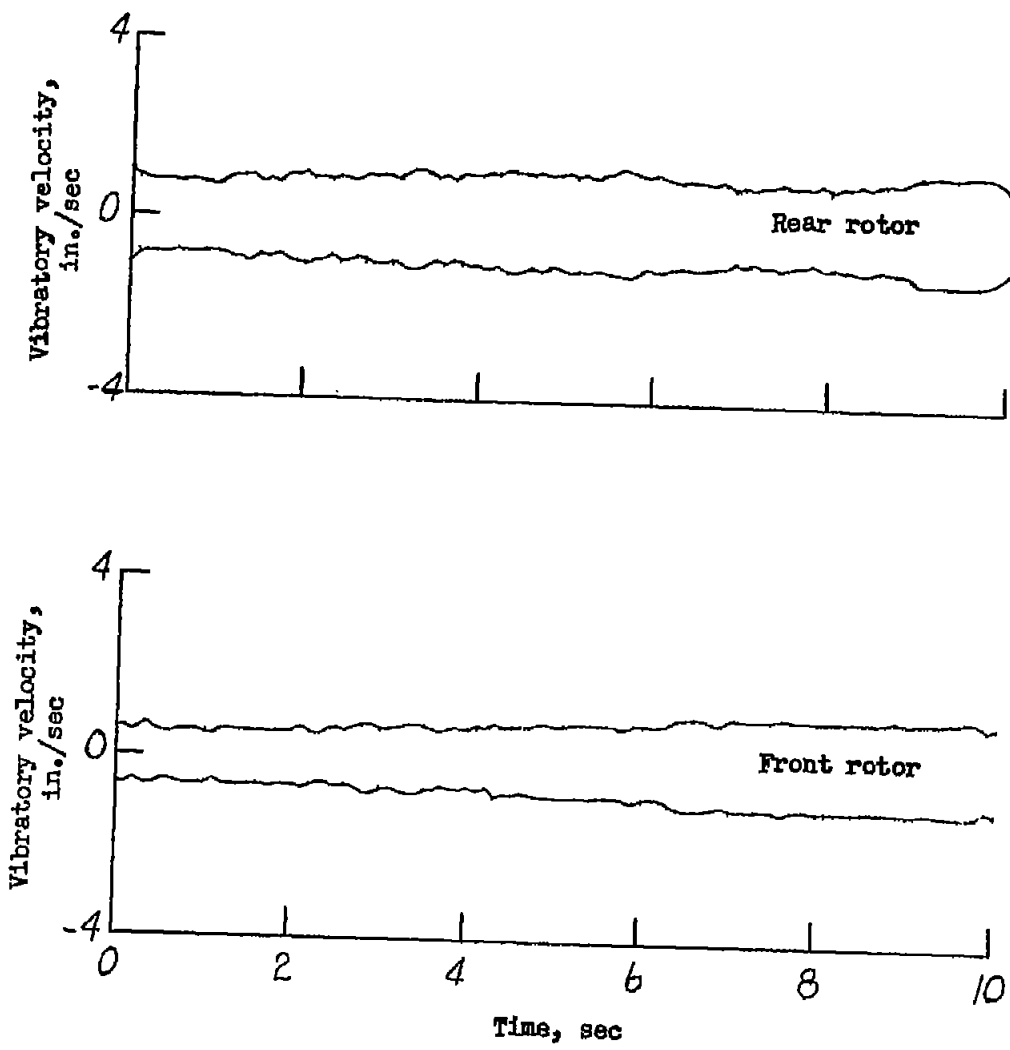


Figure 8.- Time history of the envelope of vertical vibration (containing all frequency components) measured at the front and rear rotors while the helicopter is hovering out of the region of ground effects.

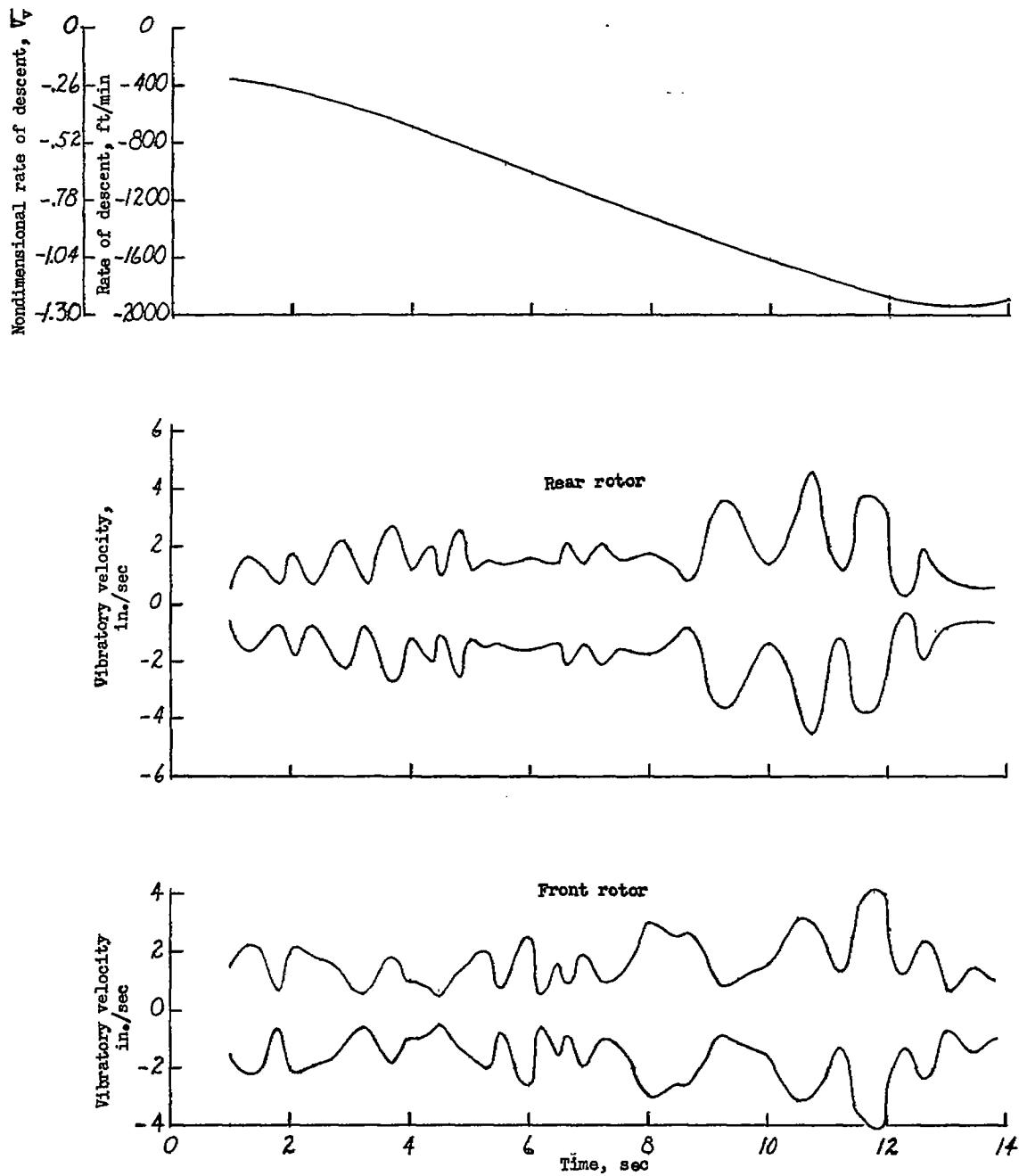


Figure 9.- Time history of the envelopes of vertical vibration (containing all frequency components) measured at the front and rear rotors while the helicopter is in the vortex-ring state at a forward speed near zero.

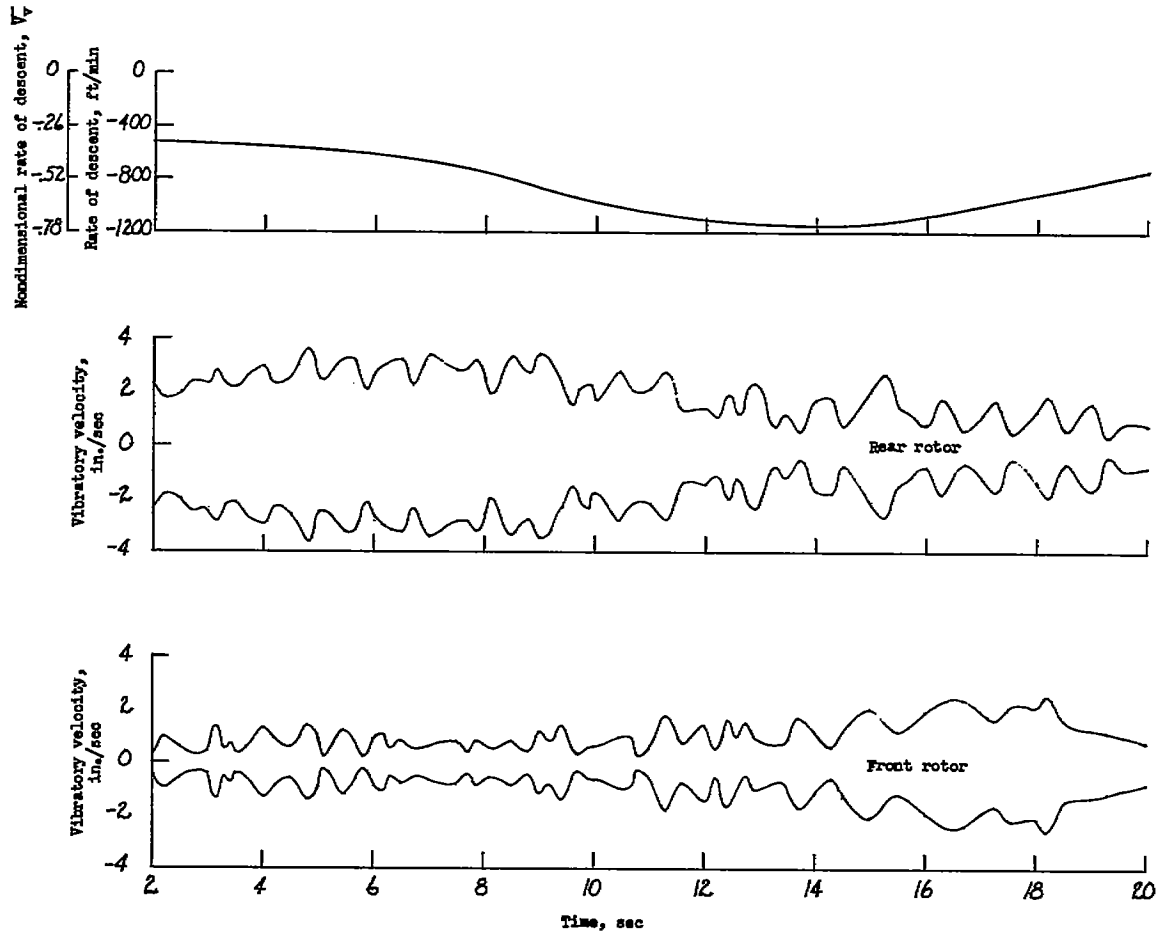


Figure 10.- Time history of the envelopes of vertical vibration (containing all frequency components) measured at the front and rear rotors while the helicopter is in the vortex-ring state at a forward speed near 10 knots.

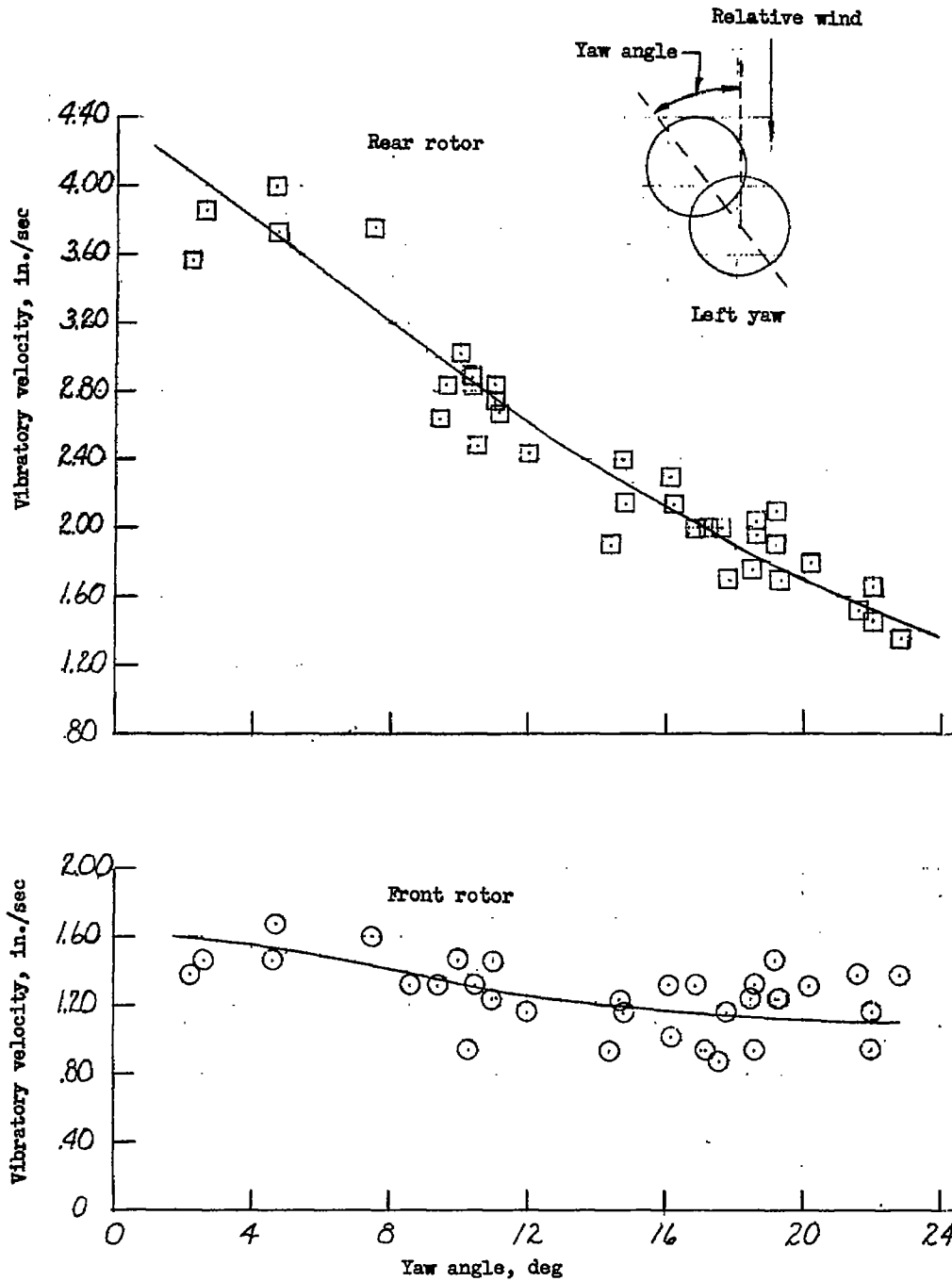


Figure 11.- Variation of vertical vibration (containing all frequency components) at the front and rear rotors while the test helicopter is yawed to the left in forward flight at 40 knots.